Research in Pharmaceutical Sciences, April 2026; 21(2): 236-250
Received: 11-05-2025
Peer Reviewed: 07-06-2025
Revised: 02-07-2025
Accepted: 24-01-2026
Published: 24-04-2026

School of Pharmacy & Pharmaceutical Sciences
Isfahan University of Medical Sciences

Original Article

PD-1: CD28 chimeric receptors enhance phenotypic and functional features of T cell subsets

Saba Feghhi-Najafabadi[1,2], Farhad Riazi-Rad[1], Mohammad Ali Shokrgozar[3], Shahriyar Abdoli[4], Fatemeh Hajari Taheri[5], Arash Arashkia[6,*], and Zahra Sharifzadeh[1,*]

[1]Department of Immunology, Pasteur Institute of Iran, Tehran, I.R. Iran. [2]Student Research Committee, Pasteur Institute of Iran, Tehran, I.R. Iran. [3]National Cell Bank of Iran, Pasteur Institute of Iran, Tehran, I.R. Iran. [4]Department of Medical Biotechnology, Faculty of Advanced Medical Technologies, Golestan University of Medical Sciences, Gorgan, I.R. Iran. [5]Food and Drug Laboratory Research Center (FDLRC), Food and Drug Administration, Iran Ministry of Health and Medical Education, Tehran. I.R. Iran. [6]Department of Molecular Virology, Pasteur Institute of Iran, Tehran, I.R. Iran.

Abstract

Background and purpose: The PD-1/PD-L1 immune checkpoint pathway inhibits T cell function, allowing tumors to escape immune responses. This study aimed to reprogram this inhibitory signaling using a PD-1:CD28 switch receptor (SR) to convert inhibitory signaling into a co-stimulatory signal and to assess its effects on the function of $CD4^+$ and $CD8^+$ T cells.

Experimental approach: PBMCs isolated from both sources were retrovirally transduced with PD-1:CD28 SR. Intracellular expression of cytokines, including IFN-γ, IL-4, IL-10, as well as the surface CD25 in $CD4^+$ and $CD8^+$ T cells, and the rate of cell apoptosis during engineering and exposure to target cells were assessed.

Findings/Results: Both buffy coat (BC) and whole blood showed comparable transduction efficiency (21.4% versus 18.5%, respectively), but BC yielded nearly double the number of viable PBMCs per 50 mL. Upon stimulation and co-culture with target cells, $CD4^+$ SR T cells produced significantly higher levels of IFN-γ, IL-4, and IL-10 compared to $CD8^+$ SR T cells. These cytokines also significantly increased in co-culture supernatants exposed to $PD\text{-}L1^+$ cells. No significant differences were found in CD4/CD8 ratios, CD25 expression, or cytokine profiles between PBMC sources. However, BC-derived T cells showed higher apoptosis rates during co-culture.

Conclusion and implications: BC can be a practical and effective source of PBMCs for T cell engineering. These findings underscore the SR signaling in the activation of $CD4^+$ T cells that may impact the activation of $CD8^+$ T cells, which is essential for effective tumor eradication.

Keywords: Blood buffy coat; CD4-positive T-lymphocytes and CD8-positive T-lymphocytes; Immunotherapy; PD-1:CD28 switch receptor; PD-L1; Whole blood.

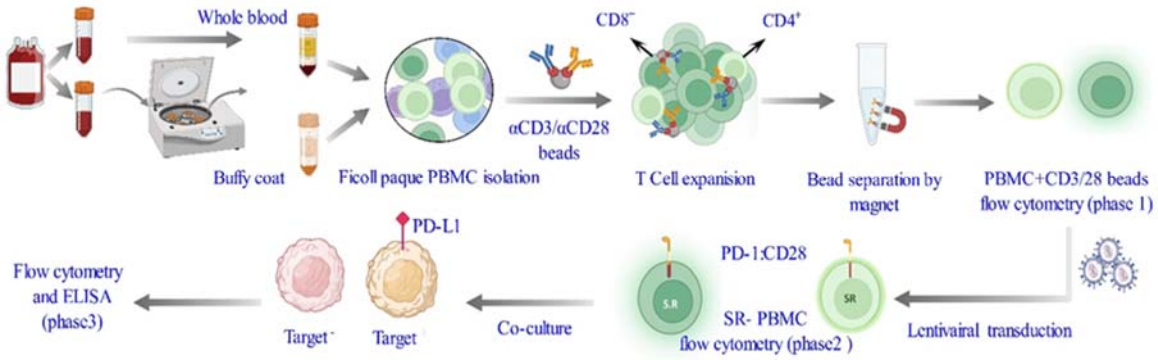

*Corresponding authors:
Z. Sharifzadeh, Tel: +98-2164112114, Fax: +98-216649259
Email: z_sharifzadeh@pasteur.ac.ir
A. Arashkia, Tel: +98-2164112338, Fax: +98-216649259
Email: arash.arashkia@gmail.com

Access this article online	
	Website: http://rps.mui.ac.ir
	DOI: 10.4103/RPS.RPS_82_25

INTRODUCTION

Adoptive T cell therapy (ACT) is a novel approach to treating cancers resistant to current standard therapies. Tumors can escape the immune system by reducing immunogenicity to limit recognition by the immune system and creating an inhibitory microenvironment to suppress the immune responses and induce T cell exhaustion (1). Factors such as chronic antigen stimulation, immunosuppressive cytokines, metabolic dysregulation, and inhibitory immune checkpoint interactions within the tumor microenvironment contribute to T cell exhaustion (2). Among these, the PD-1/PD-L1 pathway is one of the most significant contributors, playing a crucial role in tumor immune evasion and serving as a key target for cancer immunotherapy (3). The blockade of the PD-1/PD-L1 axis has revolutionized cancer therapy and is now considered a key strategy in immuno-oncology (4,5). FDA-approved monoclonal antibodies against PD-1 (nivolumab and pembrolizumab) and PD-L1 (atezolizumab or durvalumab) have shown remarkable clinical benefits in a wide range of malignancies, including non-small cell lung cancer, melanoma, and renal cell carcinoma (6). However, despite their success, immune checkpoint inhibitors (ICIs) may elicit immune-related adverse effects (irAEs), including autoimmune reactions and cytokine release syndrome (CRS), which can compromise patient safety and limit their broader application (7,8). Furthermore, many patients do not respond to therapy or eventually develop resistance, underlining the need for more precise and controllable immunotherapeutic modalities (4).

One promising next-generation immunotherapy approach involves the use of synthetic immune receptors, particularly switch receptors (SRs), which are engineered to convert inhibitory signals such as those from the PD-1/PD-L1 axis, into stimulatory signals. By fusing the extracellular domain of PD-1 with an intracellular signaling module, these receptors enable T cells to recognize and respond to PD-L1$^+$ tumor cells not with suppression, but with enhanced activation and function (9).

The intracellular signaling domain is crucial for the therapeutic efficacy and safety of SRs, with CD3ζ causing tonic signaling and activation-induced cell death (AICD), while CD28 enhances proliferation and survival, avoiding immune activation risks such as CRS or autoimmunity (10).

Designing CD28 downstream of PD-1 enhances T cell activity while preventing excessive immune responses, thereby contributing to immune balance and reducing the risk of adverse events (11). Preclinical studies have demonstrated the enhanced cytotoxicity, persistence, and tumor infiltration of SR-engineered T cells, particularly in PD-L1-rich cancers (12). Furthermore, ongoing early-phase clinical trials (NCT06084286, NCT04684459, NCT03672305, and NCT05477927) evaluated SRs in the context of CAR T-cell therapies for solid tumors, supporting their translational potential and safety in clinical settings (13). Therefore, SRs represented a rational and innovative strategy to overcome immune resistance and improve the precision and safety of current checkpoint blockade therapies (14).

The composition of T cell subsets is critical in engineered T cell therapies. CD8$^+$ cytotoxic T cells are key effectors in antitumor immunity, while CD4$^+$ T cells enhance cytotoxic T lymphocytes (CTL) function through cytokine secretion and dendritic cell modulation (15,16). CD4$^+$ cells are divided into functional subsets, including T helper 1 (Th1) and T helper 2 (Th2) cells. Th1 cells promote antitumor responses *via* interferon gamma (IFN-γ), whereas Th2 cells, producing IL-4, are linked to tumor progression. An imbalance favoring Th2 over Th1 correlates with poor prognosis in advanced cancer. IL-10-producing CD4$^+$ T cells are heterogeneous, exhibiting both regulatory and potential antitumor roles (17,18).

Recent investigation identified the various subsets of CD8$^+$ cytotoxic T cell (Tc), comparable to CD4$^+$ T cell subtypes, each containing unique effector activities and cytotoxic abilities that variably enhance antitumor immunity (19). Tc1 cells, characterized by IFN-γ production, facilitate cytotoxicity *via* perforin or Fas-dependent pathways and are pivotal in the eradication of

tumor cells. Tc2 cells release IL-4 and employ perforin-mediated cytotoxicity; yet, their role in antitumor responses seems constrained (20). Furthermore, IL-10-producing $CD8^+$ T cells demonstrated immunoregulatory capabilities by inhibiting the growth of Th1 and Th2 cells (21). The distinct functions of $CD4^+$ and $CD8^+$ T cell subsets are crucial for cancer immunotherapy, since successful approaches require the activation and synchronization of both cell types to elicit strong and lasting antitumor responses (22). CD28 co-stimulation elicits distinct responses in $CD4^+$ and $CD8^+$ T cells: $CD4^+$ T cells experience prolonged activation, proliferation, and IL-2 production, whereas $CD8^+$ T cells exhibit temporary activation, subsequent IL-2 downregulation, and heightened vulnerability to apoptosis (23). These distinctions highlight the necessity of analyzing both $CD4^+$ and $CD8^+$ subsets to evaluate the effectiveness of ACT (24).

Peripheral blood mononuclear cells (PBMCs) are the primary source of lymphocytes for the generation of genetically engineered T cells (24,25). The initial step in producing engineered T cells is isolating PBMCs, which is followed by activation, gene alteration, expansion, and performing crucial functional evaluations to evaluate their effectiveness (26). The success of *in vitro* and clinical applications depends critically on the quality and functionality of separated cells, given the important role PBMCs play in this process (27). Buffy coat (BC) and whole blood (WB) are the two primary sources for isolating PBMCs. Each source has unique characteristics influencing its suitability for specific applications, particularly in immunological research development (28).

The functionality of PBMCs is influenced by their interaction with environmental and mechanical factors during isolation and handling (29). The mechanical stress impacts various cellular processes, including T cell activation, where mechanical cues modulate the activation of T cells by influencing receptor clustering and signaling pathways, proliferation, and differentiation, leading to the development of various phenotypes, such as Th1, Th2, and regulatory T cells (Tregs) (30). The isolation of PBMCs from WB or BC involves multiple steps that can subject cells to mechanical stress. Key mechanical stressors during PBMC isolation- such as centrifugation-induced shear forces, repeated pipetting, and temperature fluctuations- can compromise cell membrane integrity, signaling pathways, and overall viability. These factors may impact the functional comparability of PBMCs isolated from WB versus BC (27,30,31).

This study investigated the frequency of $CD4^+$ T cells producing IFN-γ, IL-4, and IL-10, as well as the analogous subsets in $CD8^+$ T cells, during engineering PBMCs with PD-1:CD28 SR and when exposed to PD-$L1^+$ target cells. In addition, the effect of the source of isolated PBMCs (BC and WB) was also compared on the frequency of the cell populations during the cell engineering process.

MATERIALS AND METHODS

Switch receptor design

The SR gene construct consisted of the PD-1 signal peptide (Q15116 · PDCD1_HUMAN aa 1-24) with a c-Myc tag (EQKLISEEDL) and PD-1 extracellular domain (Q15116 · PDCD1_HUMAN aa 25-170), fused with the transmembrane and co-stimulatory domains of CD28 (P10747 · CD28 _HUMAN aa 153-220) (https://www.uniprot.org/) (Fig. 1A). The designed SR sequence was verified using CLC software, its 3D protein structure was modeled with ChimeraX 1.8, and its interaction with PD-L1 was analyzed using the HADDOCK online database (https://rascar.science.uu.nl/haddock2.4/). The designed SR gene was synthesized by GenScript (China) and first cloned into the pUC 57 plasmid. PD-1:CD28 was subcloned into the lentiviral transfer plasmid pCDH-CMV-MCS-EF1α-PURO (CD510B-1) (Addgene, USA) to generate the recombinant lentiviral transfer plasmid containing PD-1:CD28 SR. This lentiviral plasmid also encoded enhanced green fluorescent protein (EGFP), which served as a marker of SR expression. Also, the c-Myc tag was considered the surface expression recognition factor.

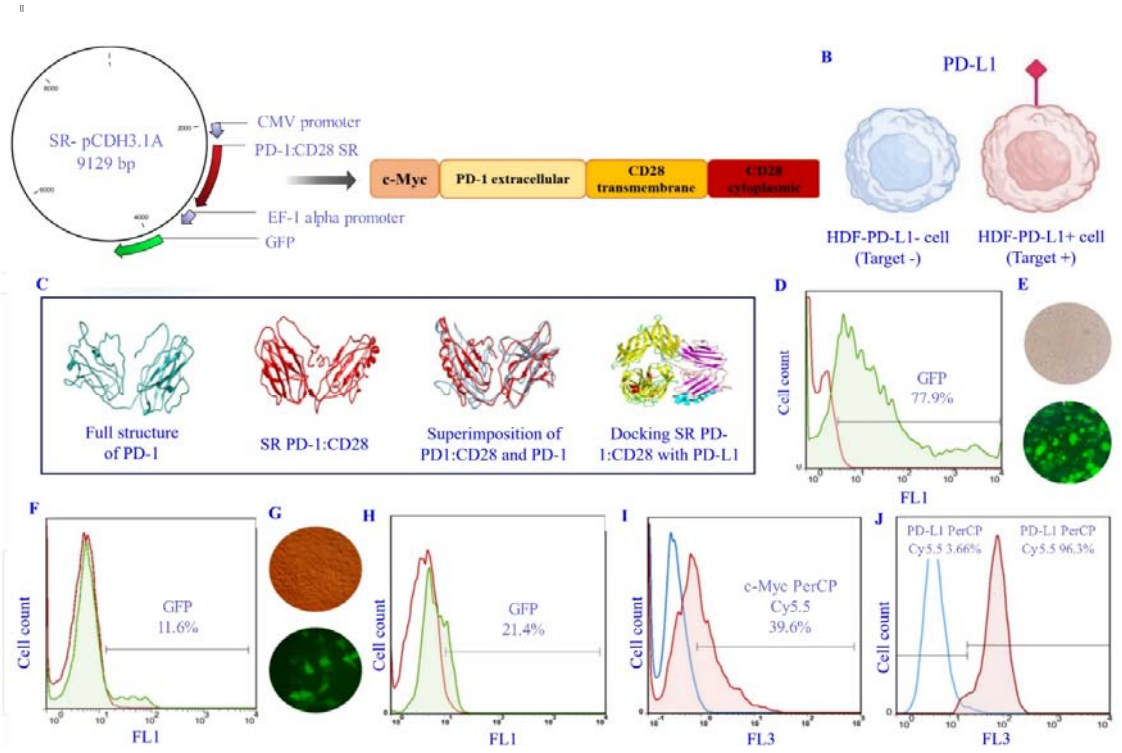

Fig. 1. Design and production of PD-1:CD28 SR. (A) Schematic representation of the pCDH3.1A vector containing the extracellular domain of PD-1 and the intracellular domain of CD28; (B) schematic diagram of target cells where HDF cells induced with IFN-γ and expressing PD-L1 were considered as positive targets (HDF-PD-L1^{+} cell), and HDF cells without induction were considered as negative targets (HDF-PD-L1^{-} cell); (C) protein structure of SR compared to PD-1 and SR docking with PD-L1; (D) flow cytometry analysis showing 77.9% GFP expression in Lenti-x cells transfected with the SR construct (FL1-GFP); (E) phase-contrast (upper) and fluorescence (lower) images confirming GFP expression in transfected cells; (F) transduction efficiency measured by GFP expression in HEK293T cells (FL1-GFP); (G) phase-contrast (upper) and fluorescence (lower) images confirming transduction efficiency in HEK293T cells; (H) flow cytometry analysis showing 21.4% GFP expression in PBMCs (FL1-GFP); (I) flow cytometry analysis of c-Myc surface expression in GFP^{+} transduced PBMCs confirming expression of the SR on the cell surface (FL3- PerCP Cy5.5); (J) flow cytometry analysis showing 96.3% PD-L1 expression in HDF cells after IFN-γ stimulation compared to 3.66% in untreated cells (FL3- PerCP Cy5.5). SR, Switch receptor; HDF, human dermal fibroblast; IFN-γ, interferon-γ; GFP, green fluorescent protein; PBMCs, peripheral blood mononuclear cells.

Isolation of PBMCs

Blood samples were collected from 6 healthy donors through the Iranian Blood Transfusion Organization (IBTO). All experiments were conducted according to the guidelines of the Ethics Committee of the Pasteur Institute of Iran (PII) with ethical code: IR.PII.AEC.1400.072. Each donor provided a single blood bag (approximately 450 mL), which was divided into 2 equal portions. One portion was used directly to isolate PBMCs as a WB sample, while the other portion was centrifuged for 10 min at 5000 *g* according to the BC separation process of the blood bank (32). PBMCs from WB and BC were rapidly isolated using standard Ficoll-Paque density gradient centrifugation protocols. The resulting PBMC pellets from both sources were resuspended in RPMI-1640 medium, supplemented with 10% fetal bovine serum (FBS), 2 mM L-glutamine, and recombinant human IL-2 (100 U/mL), at a concentration of 1 × 10^{6} cells/mL to support T-cell survival and proliferation. Cell counts were conducted with a hemocytometer (Neubauer, Marienfeld, Germany), and viability was evaluated using the trypan blue exclusion technique.

Cell lines

Isolated PBMCs were used as effector cells, and Lenti-X and HEK293T cells were employed for lentivirus production and titration, respectively. Human dermal fibroblasts (HDFs)

served as target cells. All cell lines were acquired from the National Cell Bank of Iran (NCBI) and cultured in Dulbecco's modified Eagle medium (DMEM) enriched with 10% FBS, 1% penicillin-streptomycin, and 2 mM L-glutamine at 37 °C in a humidified incubator with 5% CO_2.

Assessment and induction of PD-L1 expression on target cells

To evaluate the functionality of SR-expressing cells against PD-L1$^+$ cells, it was essential to use a cell line that did not inherently express PD-L1 as the negative control. However, this was not feasible with cancer cell lines, which typically express PD-L1. Therefore, HDF cells were employed as a model target cell. The baseline expression of PD-L1 in HDF cells was assessed to confirm their PD-L1-negative status. Additionally, PD-L1 expression was induced in HDF cells using interferon-γ (IFN-γ) to create a comparable target cell line that differed only in its PD-L1 expression levels (34). For this, HDFs were treated with recombinant human IFN-γ (50 ng/mL) using 2 consecutive doses every 2 days. PD-L1 expression was evaluated before and after IFN-γ treatment using flow cytometry with an anti-PD-L1 antibody (eBioscience, San Diego, USA) to ensure effective upregulation of PD-L1 before co-culture experiments (Fig. 1B).

Lentivirus production

Three plasmids were used to transfect virus-producing cells based on the second-generation lentivirus production system. Lenti-X cells (1.2×10^6), cultured in a 6-well tissue culture-treated plate, were transfected using the VSV-G envelope plasmid PMD2.G (Addgene, USA), the packaging plasmid psPAX2 (Addgene, USA) encoding gag-pol, and the transfer vector encoding the gene of interest, in a ratio of 1:3:3, respectively. The polyethyleneimine reagent, a cationic polymer frequently used for DNA transfection, was employed to transfect the PD-1:CD28 SR. The lentivirus-containing supernatant was harvested every 12 h for 3 days. Lentiviral particles were concentrated by ultracentrifugation for 2 h at 50000 *g*. According to the Trono Lab protocol for viral titer measurement, 64, 16, and 4 µL of viral harvest were added to HEK293T cells. Three days after transduction, green fluorescent protein (GFP)-expressing cells were identified using flow cytometry and a fluorescent microscope to measure multiplicity of infection (MOI) (14,35)). Samples displaying GFP expression below 20% were taken as acceptable.

Flow cytometry analysis

PBMCs obtained from both WB and BC samples were analyzed in 4 experimental conditions, including activation using anti-CD3 and anti-CD28 conjugated beads, transduction *via* a gene delivery system, and co-culture with target cells to determine functional properties. At each stage, we assessed key parameters, including CD3$^+$, CD4$^+$, and CD8$^+$ T cells and the frequency of CD25, IFN-γ, IL-10, and IL-4 in these cells, and also apoptosis levels. In addition, we calculated the IFN-γ/IL-4, the IFN-γ/IL-10, and the CD8/CD4 ratios. Flow cytometry analysis was performed to evaluate both surface and intracellular markers. In all staining procedures, 5×10^5 cells/tube were collected and incubated with the specified antibodies.

Following staining

For surface marker analysis, T cells were stained with PerCP/Cy7-conjugated anti-c-Myc tag (Santa Cruz Biotechnology, Texas, USA) to detect PD-1:CD28 SR surface expression, and the GFP signal was simultaneously acquired. PD-L1$^+$ tumor cells were stained with PerCP-Cy5.5-conjugated mouse anti-human PD-L1 for PD-L1 surface detection. Additionally, for each group WB and BC, cells were divided into 3 tubes as follows: 1. stained with anti-CD3 PerCP and PE-conjugated anti-CD25; 2. stained with PerCP-Cy5.5-conjugated anti-CD4 and PE-conjugated anti-CD25; 3. stained with anti-CD8 PerCP-Cy5.5 and PE-conjugated anti-CD25. For intracellular cytokine staining, PBMCs were initially surface-stained with PerCP-Cy5.5-conjugated anti-CD3, anti-CD4, and anti-CD8 antibodies, fixed with 2% (v/v) formaldehyde, and permeabilized with 0.1% (w/v) saponin. The permeabilized cells were then divided into 3 tubes to evaluate cytokine expression separately for the WB and BC groups. The tubes in each group were stained with one of the following PE-conjugated antibodies: anti-IFN-γ, anti-IL-10, or anti-IL-4 (eBioscience, San Diego, USA).

Fluorescence was assayed using a Partec PAS III (Partec GmbH, Germany), and all data were analyzed with FlowJo V10 software.

T cell expansion and lentiviral transduction

Dynabeads™ Human T Activator CD3/CD28 (Thermo Fisher Scientific) was employed to activate primary T cells at a 1:2 bead-to-cell ratio, supplemented with 100 IU/mL IL-2, throughout a three-day period preceding lentiviral transduction. The beads were subsequently extracted utilizing a magnetic separator. The media of the activated cells were substituted with lentiviral supernatant at an MOI of 10 and treated with polybrene at a concentration of 6 mg/mL in the culture media. Furthermore, T cell culture media were supplemented with 50 IU/mL IL-2 every 2 days for a duration of 72 h. To assess the efficacy of transduction *via* flow cytometry, the cell population was initially gated on GFP^+ cells, followed by an analysis of the percentage of c-Myc-positive cells within each cell population.

In vitro stimulation of SR cells and quantitation of cytokines

In the co-culture assay, target cells were plated in 48-well plates, and the transduced effector cells were introduced at an effector-to-target (E:T) ratio of 3:1. This ratio was selected based on the previous experiment demonstrating that an E:T ratio of 3:1 provided sufficient T cell activation and cytokine production while avoiding excessive cytotoxicity that may obscure differential functional responses (36). The co-culture was maintained for 24 h under standard cell culture conditions. Then, the functional phenotype of $CD4^+$ and $CD8^+$ T cells and the rate of apoptosis were assessed by flow cytometry. The co-culture supernatant was collected after 24 and 48 h and stored at -80 °C for further quantification. IL-4, IL-10, and IFN-γ levels in the culture supernatant were determined using the human IL-4 and IL-10 ELISA Set (R&D, USA) and human IFN-γ ELISA Set (Biolegend, USA).

Statistical analysis

The data were presented as mean ± SD and analyzed using GraphPad Prism software (version 10). An unpaired t-test was performed to identify differences across the treatment groups. *P*-values ≤ 0.05 were considered statistically significant.

RESULTS

Generation of SR cell using lentiviral gene transfer and PD-L1$^+$ target cell

This study investigated the feasibility of designing an SR for $PD\text{-}L1^+$ tumor cells applicable in cell-based immunotherapy. A chimeric SR was designed by fusing the signal peptide and extracellular domain of PD-1 with the transmembrane and intracellular signaling domains of CD28 (Fig. 1A). The protein and structural conformation of the SR were modeled by fusing the extracellular domain of PD-1 with the transmembrane and intracellular signaling domains of CD28. The full-length PD-1 structure was retrieved from the Protein Data Bank (PDB) and used as a reference to evaluate the modeled SR. Protein-protein docking analysis with PD-L1 was performed using the HADDOCK platform to assess binding feasibility. The analysis confirmed stable interaction between PD-1 and PD-L1 in the context of the SR, supporting the structural integrity and functional compatibility of the engineered receptor (Fig. 1C). The construct transfection efficiency was assessed by flow cytometry (Fig. 1D) and fluorescence microscopy (Fig. 1E), based on GFP expression as a reporter, which showed a high transfection rate of 77.9%.

Lentiviral particles were produced and titrated in HEK293T cells according to the Trono lab protocol (35). In this study, a 16 µL aliquot of viral harvest with a transduction efficiency of 11%- within the recommended range of less than 20%- was selected for viral titer determination. Based on this, the viral titer was estimated to be approximately 9×10^6 TU/mL. This value was subsequently used to calculate the required volume of viral supernatant to achieve an MOI of 10, which was then added to the PBMCs (Fig. 1F and G). To evaluate the efficiency of transduction in PBMCs by flow cytometry, both WB and BC groups underwent lentiviral transduction. No notable disparity was detected in transduction efficiency between both groups, with mean

GFP$^+$ cell percentages of 18.5% for the WB group and 21.4% for the BC group (Fig. 1H). To verify surface localization of the receptor, c-Myc expression was analyzed within the GFP$^+$ population using flow cytometry. The results demonstrated that 39.6% of the transduced cells expressed the SR on the BC surface (Fig. 1I). To validate PD-L1 expression and investigate the effect of IFN-γ on its induction, HDF cells were treated with IFN-γ, and PD-L1 surface expression was analyzed using flow cytometry. The results indicated that, after induction, over 96% of cells expressed PD-L1 compared to 3.66% in the untreated group (Fig. 1J). This notable distinction significantly confirmed the appropriateness of these cells as the target cells in subsequent research.

Comparative analysis of the behavior of T cell subsets in engineering and co-culture processes based on the PBMC source

In the first step, the effect of mechanical stresses during the processing of PBMCs from different sources (BC versus WB) on T cell phenotype and function was investigated. For this purpose, a comprehensive assessment of the quality and phenotype of engineered T cells was performed by measuring key immune parameters, including the frequency of CD4$^+$ and CD8$^+$ T cell populations, the apoptosis rate in cells, the frequency of CD25$^+$ cells (a marker of activated cells), and the frequency of cells producing the cytokines IFN-γ (a marker cytokine of Th1 and Tc1 groups), IL-4 (a marker cytokine of Th2 and Tc2 subgroups), and IL-10 (an inhibitory cytokine produced by regulatory cells) at all stages of engineering and co-culture in PBMCs isolated from BC and WB. To better understand the results, the CD8/CD4, IFN-γ/IL-4, and IFN-γ/IL-10 ratios were used to compare the BC and WB results. This integrated analysis allowed us to identify the impact of both T cell subset composition and PBMC source on the efficacy and reliability of SR expression and functional outcomes.

During the PBMC isolation step, approximately 50 × 10^6 viable cells were obtained from 50 mL of WB, whereas the same volume of BC yielded around 100 × 10^6 viable PBMCs, indicating a significantly higher cell yield from the BC compared to the WB.

The frequency of apoptotic cells in cells isolated from BC was higher in the CD3/CD28 bead stimulation, co-culture with PD-L1$^-$ target, and PD-L1$^+$ target stages than those in WB (Fig. 2A). No significant differences were observed in the frequency of CD25$^+$ cells (Fig. 2B) and the ratios of IFN-γ/IL-10 (Fig. 2C) and IFN-γ/IL-4 (Fig. 2D) between PBMCs from WB and BC during the engineering process and co-culture with target cells. Following PBMC isolation by Ficoll, the initial CD8:CD4 ratio was approximately 1:2 (data not shown), but after stimulation with CD3/CD28 beads, this ratio shifted to about 2:1, indicating the preferential CD8$^+$ expansion. However, no significant difference in the CD8/CD4 ratio was observed between BC and WB sources in the subsequent phases of the study. (Fig. 2E). In general, irrespective of the apoptosis level, the findings from the BC group seemed to be analogous to those of WB.

Functional activity and cytokine secretion of SR cells in response to PD-L1$^+$ target cells

In the next step, the effect of PD-1:CD28 SR signaling on effector CD4$^+$ and CD8$^+$ T cell subsets was assessed after exposure to PD-L1$^+$ and PD-L1$^-$ targets. Flow cytometry analysis was performed at each stage of the experiment, and representative results for CD25 expression were presented in Fig. 3A as an example. The percentage of IL-10$^+$ (Fig. 3B) and IFN-γ$^+$ (Fig. 3C) cells in CD4$^+$ T cells was significantly increased when co-cultured with PD-L1$^+$ cells compared to PD-L1$^-$ cells. No significant difference was observed in the frequency of IL-4$^+$ (Fig. 3D) and CD25$^+$ (Fig. 3E) cells in CD4$^+$ and CD8$^+$ T cells between Target$^+$ and Target$^-$ groups. However, the ratios of IFN-γ/IL-4$^+$ (Fig. 3F) and IFN-γ/IL-10$^+$ (Fig. 3G) did not differ in CD4$^+$ and CD8$^+$ T cells when co-cultured with Target$^+$ and Target$^-$. Cytokine measurement in the supernatant of the cells co-cultured with Target$^+$ and Target$^-$ showed a significant increase in the production of IFN-γ, IL-4, and IL-10 in the Target$^+$ group compared with the Target$^-$ group at both 24 h (Fig. 3H) and 48 h (Fig. 3I) post co-culture.

Comparable tests were performed on T cells obtained from the WB group; however, due to the absence of statistically significant differences between the results of WB and BC, only the findings from the BC group were reported here.

Differential cytokine expression and activation signatures of CD4$^+$ and CD8$^+$ SR cells upon engagement with PD-L1$^+$ target cells

To compare PD-1:CD28 SR signaling in CD4$^+$ and CD8$^+$ T cells in the presence of target cells, the frequency of IL-4, IL-10, and IFN-γ producing cells and CD25 expressing effector cells was compared in these two cell populations after co-culture with PD-L1$^+$ and PD-L1$^-$ cells (Fig. 4A). The results showed that the frequency of IL-4, IL-10, and IFN-γ-producing cells significantly increased in CD4$^+$ T cells in response to PD-1:CD28 SR signaling compared to CD8$^+$ T cells. However, no significant differences were observed in the IFN-γ/IL-10$^+$ and IFN-γ/IL-4$^+$ ratios between the two subsets (Fig. 4B). A strong positive correlation was observed among the IFN-γ/IL-10 and IFN-γ/IL-4 ratios within both CD8$^+$ and CD4$^+$ T cell subsets (Pearson's r > 0.98 for all comparisons), indicating highly coordinated cytokine expression profiles across these immune populations.

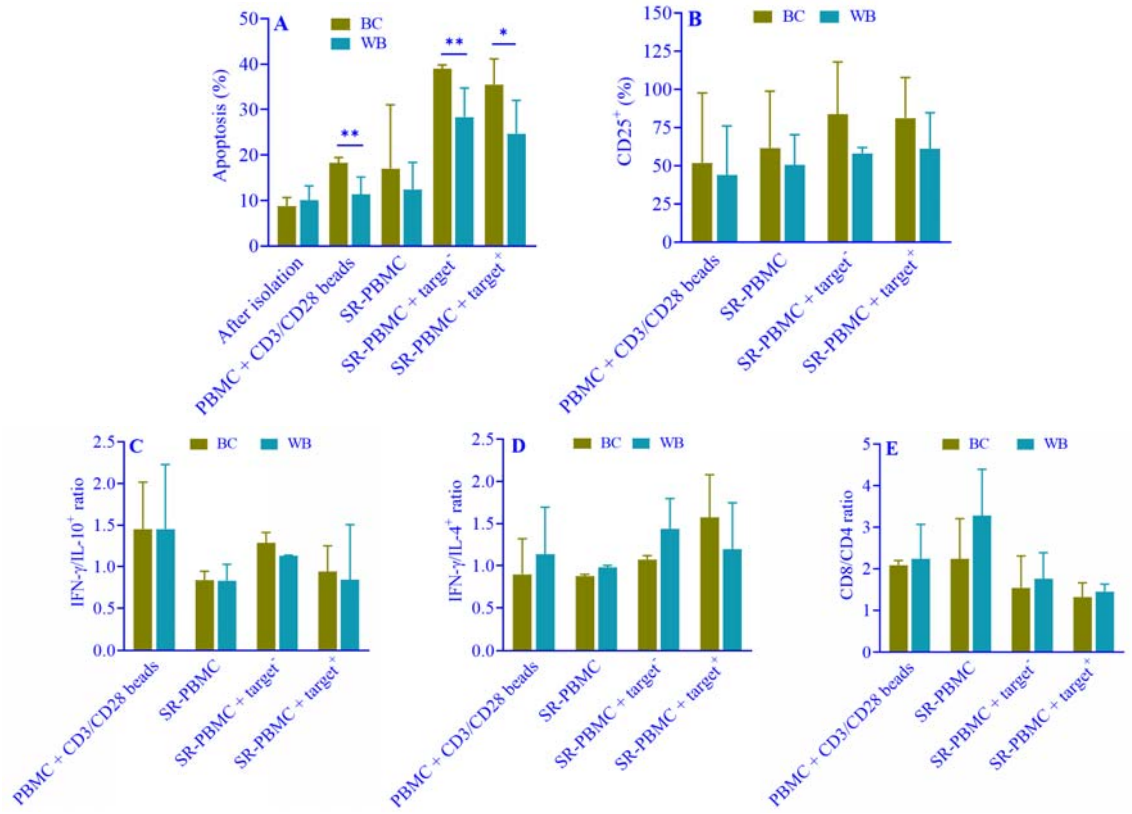

Fig. 2. Comparison of phenotype and function of T cells derived from WB and BC in response to target cells. (A) Apoptosis percentage; (B) CD25 expression; (C) IFN-γ/IL-10 ratio; (D) IFN-γ/IL-4 ratio; (E) CD8/CD4 ratio. Statistical analysis was performed using an unpaired t-test for comparisons between treatment groups. Data were expressed as mean ± SD. $^*P < 0.05$ and $^{**}P < 0.01$ demonstrate significant differences between respective groups. WB, Whole blood; BC, buffy coat; IFN-γ, interferon-γ; IL, interleukin.

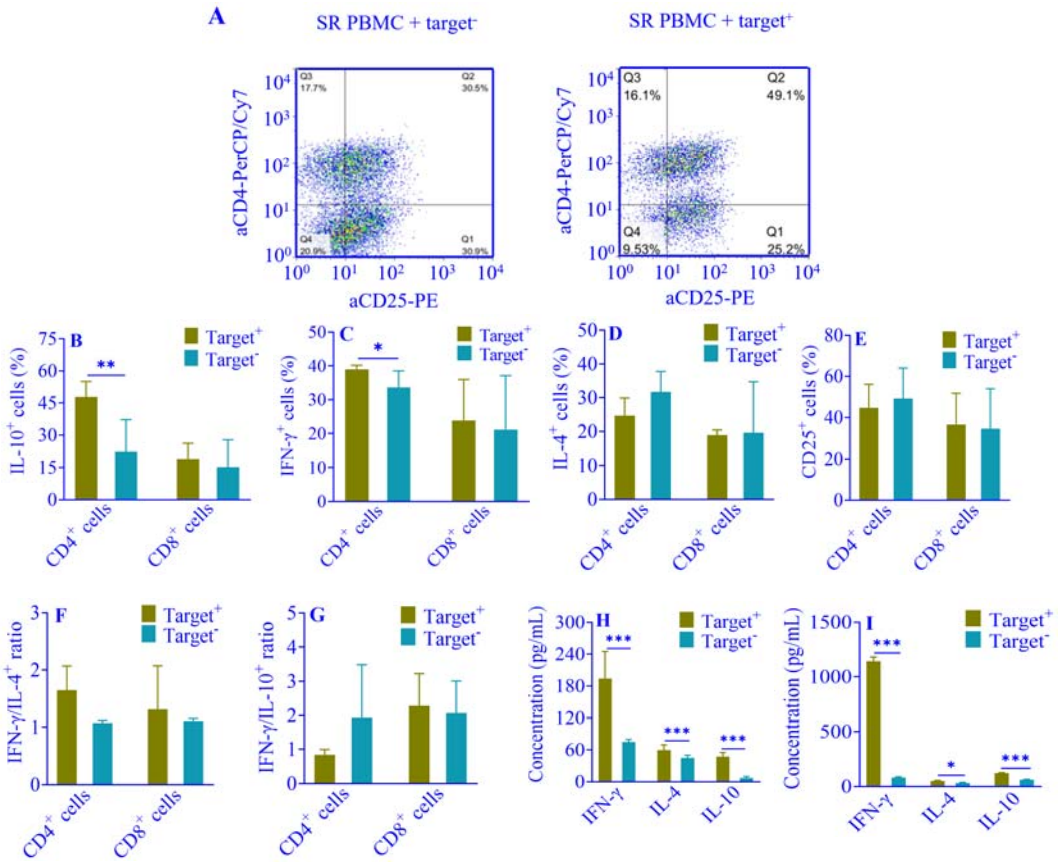

Fig. 3. Cytokine secretion profile and activation status of SR-PBMCs (BC source) following target cell co-culture. **(**A) Representative flow cytometry dot plots for CD25 and CD4 expression across both experimental conditions of SR-PBMCs with PD-L1^{-} target (target^{-}) and SR-PBMCs co-cultured with PD-L1^{+} target cells (target^{+}). Y axes show FL3 channel and PerCP/CY5 fluorochrome, and X axes show FL2 and PE fluorochrome; (B) IL-10, (C) IFN-γ, (D) IL-4, and (E) CD25 expression in CD4^{+} and CD8^{+} T cell subsets; (F) IFN-γ/IL-4 and (G) IFN-γ/IL-10 ratios in both CD4^{+} and CD8^{+} T cells, indicating a shift in Th1/Th2 and inflammatory/regulatory balance; concentration of cytokines including IFN-γ, IL-4, and IL-10 measured in the culture supernatant using ELISA after (H) 24 h and (I) 48 h co-culture with PD-L1^{+} targets. Statistical analysis was performed using an unpaired t-test for comparisons between treatment groups. Data were expressed as mean ± SD. $^{*}P < 0.05$, $^{**}P < 0.01$, and $^{***}P < 0.001$ demonstrate significant differences between respective groups. IFN-γ, Interferon-γ; IL, interleukin; PBMCs, peripheral blood mononuclear cells.

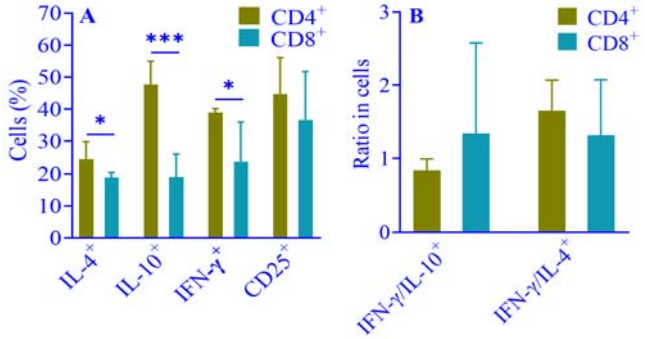

Fig. 4. Cytokine and activation marker expression in CD4^{+} and CD8^{+} T cells upon co-culture with PD-L1^{+} target cells. (A) The percentage of intracellular IFN-γ, IL-4, IL-10, and CD25 expressing cells and (B) the IFN-γ/IL-4 and IFN-γ/IL-10 ratios. Statistical analysis was performed using an unpaired t-test for comparisons between treatment groups. Data were expressed as mean ± SD. $^{*}P < 0.05$ and $^{***}P < 0.001$ demonstrate significant differences between respective groups. IFN-γ, Interferon-γ; IL, interleukin.

DISCUSSION

PD-1 is a pivotal immune checkpoint molecule that inhibits anti-tumor effector responses and is essential for the management of advanced cancer patients (ACP). The engagement of PD-1 on T cells with its ligand PD-L1 on tumor cells facilitates clonal deletion and T cell exhaustion, resulting in immunological suppression (37). Tumors evade immune surveillance by downregulating CD28 ligands on their surface, a process that may also be promoted by tolerogenic processes affecting tumor-specific T cells (38). Additionally, active T cells inherently reduce CD28 expression as a natural feedback mechanism to regulate immunological responses (39). Previous investigation indicated that the intratumoral induction of B7-1 (CD80), a ligand for CD28, can augment T cell responses and facilitate tumor regression (40). We developed a PD-1:CD28 SR to transform the inhibitory signals from PD-1/PD-L1 interactions into a stimulatory signal mediated by CD28, based on this evidence. This study examined the impact of the chimeric receptor on the activation of $CD4^+$ and $CD8^+$ T cell subsets when exposed to PD-L1-expressing target cells without antigen-specific stimulation. This study investigated the impact of the source of PBMCs from WB or BC and the stress conditions during isolation on the phenotype and transduction efficiency of engineered T cells. The results clarified how cellular background affected the functional outcomes of T cell engineering with PD-1:CD28 SRs.

High-quality PBMCs in clinical trials serve as an essential resource for generating functional T cells and maintaining the stability of cell subsets (41). While both WB and BC serve as common sources for PBMC isolation, they differ significantly in cellular yield and processing demands. WB contains all blood components, which may dilute the concentration of the cells of interest, whereas the BC represents an enriched fraction predominantly consisting of PBMCs and platelets (42). The current data indicated that for equal volume, the cell yield in BC was twice that of WB.

However, the additional handling steps required for BC processing, such as centrifugation and extensive pipetting, may introduce mechanical stress that negatively impacts the survival and functionality of T cells. The apoptotic profiles of PBMCs from WB and BC become increasingly similar after Ficoll preparation. Consistent with this, Szczepiorkowski *et al*. indicated that physical stress does not induce apoptosis in the BC cells (43). In the present study, although the CD8/CD4 ratio and the frequency of $CD25^+$ cells (a marker of T cell activation) were similar between PBMCs derived from WB and BC, we observed a significantly higher rate of apoptosis in BC-derived T cells following CD3/CD28 stimulation and co-culture with $PD\text{-}L1^-$ and $PD\text{-}L1^+$ targets. Although no significant difference in apoptosis levels was observed between PBMCs derived from BC and WB following Ficoll isolation and lentiviral transduction, a statistically significant difference emerged upon co-culture with $PD\text{-}L1^+$ target cells.

The comparison of effector cell frequency between PBMCs derived from BC and WB in different phases of engineering and co-culture indicated that although the effector cell ratios were comparable, the frequency of effector cells, particularly those producing IFN-γ, was significantly increased in BC compared to WB upon stimulation (CD3/CD28 beads and co-culture) (data not shown). IFN-γ can induce apoptosis in activated T cells (44,45), which is dependent on the mitochondrial pathway of apoptosis (46). Therefore, increased apoptosis in BC-derived T cells could be due to an increase in activated cells and IFN-γ, suggesting additional investigation in the future. $CD4^+$ T cells, rather than $CD8^+$ T cells, are recognized as the primary mediators of cytokine release syndrome (CRS). Previous research has highlighted the significance of sustaining a CD4:CD8 ratio close to 1:1 to optimize antitumor synergy, whereas increased ratios (exceeding 1.12) have been associated with weaker treatment results (47). Interestingly, the current study showed that the initial CD4:CD8 ratio was approximately 2:1. However, upon CD3/CD28 stimulation, this ratio shifted to roughly 1:2, reflecting the preferential expansion of $CD8^+$ T cells. This reversal persisted throughout the downstream processes, potentially contributing to reduced

CRS risk while preserving the cytotoxic potency of the T cell product. These findings suggested that CD3/CD28 stimulation not only enhances activation but may also steer the T cell composition toward a functionally favorable profile for adoptive cell therapy.

To facilitate the comparison of effector populations at various stages of SR-PBMC cell engineering and co-culture with targets, the ratios of IFN-γ/IL-10 and IFN-γ/IL-4 cytokines were assessed. No differences in these ratios were observed during the study phases, indicating that the PBMC sources did not affect lymphocyte phenotypes. According to the present results, this study suggests BC as a feasible and practical source for the isolation of PBMCs, which can replace the WB.

Antitumor immune responses are mostly mediated by $CD8^+$ cells activated by Th1 cells that secrete IFN-γ. Nonetheless, despite variations in the Th1/Th2 ratio across different tumors, research indicated that the Th1 response is predominantly inhibited in the majority of cancer cases (18). Bos *et al.* demonstrated that in the tumor microenvironment, the recruitment, proliferation, and effector function of $CD8^+$ T cells are augmented by IFN-γ and IL-2 secreted by $CD4^+$ T cells (48). The elevation of this ratio in $CD4^+$ T cells in response to a PD-L1-expressing target cell in BC-derived PD-1:CD28 SR cells may confer a benefit for this cellular source. Numerous studies indicated that PD-1:CD28 receptor switch signaling results in the activation and secretion of IFN-γ from $CD4^+$ and $CD8^+$ T cells (49,50). The present study investigated, for the first time, the influence of PD-1:CD28 SR signaling on cytokine production of IFN-γ, IL-4, and IL-10 in $CD4^+$ and $CD8^+$ T cells interacting with PD-$L1^+$ and PD-$L1^-$ target cells. Although no significant variations were seen in the percentage of $CD25^+$ cells among $CD4^+$ and $CD8^+$ T cell subsets between PD-$L1^+$ and PD-$L1^-$ co-cultures, a marked elevation of IFN-γ^+ and IL-10^+ $CD4^+$ T cells was observed in response to PD-$L1^+$ targets. PD-1:CD28 SR signaling appears to more effectively activate $CD4^+$ T cells compared to $CD8^+$ T cells, and these $CD4^+$ T cells may influence the phenotypes of $CD8^+$ T cells.

One study indicated that in activated $CD8^+$ T cells exhibiting diminished CD28 expression, and in this situation, NKG2D signaling functions as a co-stimulatory signal, enhancing levels of IFN-γ and TNF-α (51). NKG2D ligands are frequently expressed by tumor cells (52), facilitating the elimination of cancer cells by $CD8^+$ T cells in animal models that express these ligands (53). The absence of notable variations in cytokine-producing cells between co-cultured PD-$L1^+$ and PD-$L1^-$ target cells may result from the participation of NKG2D and its ligands in the PD-$L1^-$ target, which compensates for PD-1:CD28 SR signaling in PD-$L1^+$ target cells. This conclusion aligns with Prosser's study, which revealed no significant change in the frequency of IFN-γ^+ $CD8^+$ T cells between PD-$L1^+$ and PD-$L1^-$ cells (49).

In pathogenic and inflammatory tumor conditions, IFN-γ within the tumor microenvironment promotes PD-L1 expression on tumor cell surfaces and diminishes NKG2D expression on $CD8^+$ T cells (54). Thus, PD-1:CD28 SR signaling seems capable of activating $CD8^+$ T cells in this environment.

The ELISA results indicated a markedly significant elevation in cytokine secretion within the supernatants of PD-$L1^+$ target cells relative to PD-$L1^-$ cells. This finding aligns with the study that, despite no discernible difference in cell frequency *via* flow cytometry, demonstrated that IFN-γ secretion was significantly greater in the PD-$L1^+$ cell group compared to the PD-$L1^-$ group (49). $CD4^+$ T cells play a crucial role in orchestrating antitumor immune responses, making their presence indispensable in CAR-T cell therapy. Lee *et al.* demonstrated that $CD4^+$ T cells directly influenced $CD8^+$ T cell activation during *ex vivo* CAR-T expansion, independent of antigen-presenting cells (APCs) (55), although $CD4^+$ CAR-T cells tended to exhibit a more exhausted phenotype. Nevertheless, they are capable of mediating cytotoxicity through IFN-γ-dependent mechanisms (56). This study revealed a strong correlation between the IFN-γ/IL-4 and IFN-γ/IL-10 ratios within both $CD4^+$ and $CD8^+$ T cell populations. Notably, the frequency of IFN-γ^+ and IL-10^+ cells was significantly higher in $CD4^+$ T cells than in $CD8^+$ T cells upon interaction with PD-$L1^+$

target cells, suggesting that activated $CD4^+$ T cells may influence $CD8^+$ T cell phenotype through PD-1:CD28 SR. Furthermore, the levels of IFN-γ and IL-10 in co-culture supernatants increased substantially at 48 h compared to 24 h post-co-culture with $PD\text{-}L1^+$ targets. While IL-10 is traditionally known for its immunosuppressive functions, emerging evidence indicates that IL-10-producing $CD4^+$ T cells can enhance mitochondrial activity, oxidative phosphorylation, and tumor infiltration, thereby improving the persistence and efficacy of IL-10-expressing CAR-T cells (57). This mechanism is associated with resistance to T cell dysfunction and sustained clearance of solid tumors and metastases. Together, these findings underscored the central role of $CD4^+$ T cells in regulating CAR-T function and highlight their therapeutic potential in improving responses against solid tumors (58,59).

Collectively, these data emphasized the pivotal role of SR function and showed their therapeutic potential in enhancing responses to solid malignancies.

CONCLUSION

The present study findings indicated that BC serves as a viable and effective source for PBMC isolation in T cell engineering. BC is less susceptible to adverse effects on function and phenotype due to the brief interaction of immune cells, particularly T cells, with RBCs. The quantity of effector cells, particularly IFN-γ-producing cells in T cells separated from BC following stimulation (CD3/CD28 beads and co-culture) showed a significant rise compared with WB, despite the ratio of these effector cells remaining similar. The elevated apoptosis observed in this context may result from the apoptosis of T cells induced by IFN-γ. Moreover, these data supported the hypothesis that showed engineered T cells elicited a robust type 1 response (characterized by elevated IFN-γ secretion) in reaction to SR signaling. Furthermore, $CD4^+$ T cells exhibited a more pronounced response to SR signaling compared to $CD8^+$ T cells and, as primary IFN-γ-secreting cells, can modulate $CD8^+$ responses.

Acknowledgments

This research was financially supported by a Ph.D. thesis grant (No. BD-9894) from the Pasteur Institute of Iran. In addition, this work was based on research funded by the Iran National Science Foundation (INSF) under project No. 4012783.

Conflicts of interest statement

All authors declared no conflict of interest in this study.

Authors' contributions

S. Feghhi-Najafabadi contributed to conceptualization, investigation, methodology, software, and writing the original draft; F. Riazi-Rad contributed to conceptualization, methodology, validation, and writing-review and editing; M.A. Shokrgozar contributed to resources and project administration; S. Abdoli contributed to software, data curation, and methodology; F. Hajari Taheri contributed to resources; A. Arashkia contributed to supervision and writing-review and editing; Z. Sharifzadeh contributed to conceptualization, funding acquisition, project administration, supervision, and writing-review and editing. All authors have read and approved the finalized article. Each author has fulfilled the authorship criteria and affirmed that this article represents honest and original work.

AI declaration

During the preparation of this work, the authors used Quillbot to improve readability and language. After using this tool, the authors reviewed and edited the content and take full responsibility for the content of the publication.

REFERENCES

1. Kim SK, Cho SW. The evasion mechanisms of cancer immunity and drug intervention in the tumor microenvironment. Front Pharmacol. 2022;13:868695,1-16. DOI: 10.3389/fphar.2022.868695.
2. Rahimmanesh I, Khanahmad H. Chimeric antigen receptor-T cells immunotherapy for targeting breast cancer. Res Pharm Sci. 2021;16(5):447-454. DOI: 10.4103/1735-5362.323911.
3. Chow A, Perica K, Klebanoff CA, Wolchok JD. Clinical implications of T cell exhaustion for cancer

immunotherapy. Nat Rev Clin Oncol. 2022;19(12):775-790.
DOI: 10.1038/s41571-022-00689-z.
4. Ribas A, Wolchok JD. Cancer immunotherapy using checkpoint blockade. Science. 2018;359(6382):1350-1355.
DOI: 10.1126/science.aar4060.
5. Nejati M, Soheili M, Salami M, Khedri M. The effect of redox bacteria on the programmed cell death-1 cancer immunotherapy. Res Pharm Sci. 2024;19(2):228-237.
DOI: 10.4103/RPS.RPS_28_23.
6. Gandhi L, Rodríguez-Abreu D, Gadgeel S, Esteban E, Felip E, Angelis FD, *et al*. Pembrolizumab plus chemotherapy in metastatic non-small-cell lung cancer. N Engl J Med. 2018;378(22):2078-2092.
DOI: 10.1056/NEJMoa1801005.
7. Postow MA, Sidlow R, Hellmann MD. Immune-related adverse events associated with immune checkpoint blockade. N Engl J Med. 2018;378(2):158-168.
DOI: 10.1056/NEJMra1703481.
8. Maali A, Noei A, Feghhi-Najafabadi S, Sharifzadeh Z. A systematic review on the dual role of interleukin-1 in CAR T-cell therapy: enhancer and mitigator. Iran Biomed J. 2024;28(5&6):221-234.
DOI: 10.61186/ibj.4444.
9. Kobold S, Grassmann S, Chaloupka M, Lampert C, Wenk S, Kraus F, *et al*. Impact of a new fusion receptor on PD-1-mediated immunosuppression in adoptive T cell therapy. J Natl Cancer Inst. 2015;107(8):djv146,1-10.
DOI: 10.1093/jnci/djv146.
10. Velasco Cárdenas RMH, Brandl SM, Meléndez AV, Schlaak AE, Buschky A, Peters T, *et al*. Harnessing CD3 diversity to optimize CAR T cells. Nat Immunol. 2023;24(12):2135-2149.
DOI: 10.1038/s41590-023-01658-z.
11. Hui E, Cheung J, Zhu J, Su X, Taylor MJ, Wallweber HA, *et al*. T cell costimulatory receptor CD28 is a primary target for PD-1-mediated inhibition. Science. 2017;355(6332):1428-1433.
DOI: 10.1126/science.aaf1292.
12. Tay JC, Zha S, Wang S. Chimeric switch receptor: switching for improved adoptive T-cell therapy against cancers. Immunotherapy. 2017;9(16):1339-1349.
DOI: 10.2217/imt-2017-0103.
13. Liu X, Ranganathan R, Jiang S, Fang C, Sun J, Kim S, *et al*. A chimeric switch-receptor targeting PD1 augments the efficacy of second-generation CAR T-Cells in advanced solid tumors. Cancer Res. 2016;76(6):1578-1590.
DOI: 10.1158/0008-5472.CAN-15-2524.
14. Liu H, Lei W, Zhang C, Yang C, Wei J, Guo Q, *et al*. CD19-specific CAR T cells that express a PD-1/CD28 chimeric switch-receptor are effective in patients with PD-L1-positive B-cell lymphoma. Clin Cancer Res. 2021;27(2):473-484.
DOI: 10.1158/1078-0432.CCR-20-1457.
15. Borst J, Ahrends T, Bąbała N, Melief CJM, Kastenmüller W. $CD4^+$ T cell help in cancer immunology and immunotherapy. Nat Rev Immunol. 2018;18(10):635-647.
DOI: 10.1038/s41577-018-0044-0.
16. Bove C, Maher J, Glover M. The role of $CD4^+$ CAR T cells in cancer immunotherapy. Transl Cancer Res. 2024;13(5):2580-2586.
DOI: 10.21037/tcr-23-2044.
17. Kravtsov DS, Erbe AK, Sondel PM, Rakhmilevich AL. Roles of $CD4^+$ T cells as mediators of antitumor immunity. Front Immunol. 2022;13:972021,1-9.
DOI: 10.3389/fimmu.2022.972021.
18. Shurin MR, Lu L, Kalinski P, Stewart-Akers AM, Lotze MT. Th1/Th2 balance in cancer, transplantation and pregnancy. Springer Semin Immunopathol. 1999;21(3):339-359.
DOI: 10.1007/BF00812261.
19. Paul MS, Ohashi PS. The roles of $CD8^+$ T cell subsets in antitumor immunity. Trends Cell Biol. 2020;30(9):695-704.
DOI: 10.1016/j.tcb.2020.06.003.
20. Dobrzanski MJ, Reome JB, Hollenbaugh JA, Dutton RW. Tc1 and Tc2 effector cell therapy elicit long-term tumor immunity by contrasting mechanisms that result in complementary endogenous type 1 antitumor responses. J Immunol. 2004;172(3):1380-1390.
DOI: 10.4049/jimmunol.172.3.1380.
21. Inoue T, Asano Y, Matsuoka S, Furutani-Seiki M, Aizawa S, Nishimura H, *et al*. Distinction of mouse $CD8^+$ suppressor effector T cell clones from cytotoxic T cell clones by cytokine production and CD45 isoforms. J Immunol. 1993;150(6):2121-2128.
PMID: 8450205.
22. Tay RE, Richardson EK, Toh HC. Revisiting the role of $CD4^+$ T cells in cancer immunotherapy-new insights into old paradigms. Cancer Gene Ther. 2021;28(1-2):5-17.
DOI: 10.1038/s41417-020-0183-x.
23. Laux I, Khoshnan A, Tindell C, Bae D, Zhu X, June CH, *et al*. Response differences between human CD4(+) and CD8(+) T-cells during CD28 costimulation: implications for immune cell-based therapies and studies related to the expansion of double-positive T-cells during aging. Clin Immunol. 2000;96(3):187-197.
DOI: 10.1006/clim.2000.4902.
24. Morgan RA, Dudley ME, Wunderlich JR, Hughes MS, Yang JC, Sherry RM, *et al*. Cancer regression in patients after transfer of genetically engineered lymphocytes. Science. 2006;314(5796):126-129.
DOI: 10.1126/science.1129003.
25. Tumeh PC, Koya RC, Chodon T, Graham NA, Graeber TG, Comin-Anduix B, *et al*. The impact of *ex vivo* clinical grade activation protocols on human T-cell phenotype and function for the generation of genetically modified cells for adoptive cell transfer therapy. J Immunother. 2010;33(8):759-768.
DOI: 10.1097/CJI.0b013e3181f1d644.
26. Rahimmanesh I, Totonchi M, Khanahmad H. The challenging nature of primary T lymphocytes for transfection: effect of protamine sulfate on the transfection efficiency of chemical transfection reagents. Res Pharm Sci. 2020;15(5):437-446.
DOI: 10.4103/1735-5362.297846.

27. Abraham RA, Agrawal PK, Acharya R, Sarna A, Ramesh S, Johnston R, *et al*. Effect of temperature and time delay in centrifugation on stability of select biomarkers of nutrition and non-communicable diseases in blood samples. Biochem Med (Zagreb). 2019;29(2):020708,1-13. DOI: 10.11613/BM.2019.020708.
28. Kizhakeyil A, Ong ST, Fazil MHUT, Chalasani MLS, Prasannan P, Verma NK. Isolation of human peripheral blood T-lymphocytes. Methods Mol Biol. 2019;1930:11-17. DOI: 10.1007/978-1-4939-9036-8_2.
29. Rushdi M, Li K, Yuan Z, Travaglino S, Grakoui A, Zhu C. Mechanotransduction in T cell development, differentiation and function. Cells. 2020;9(2):364,1-22. DOI: 10.3390/cells9020364.
30. Hashimoto Y, Kinoshita N, Greco TM, Federspiel JD, Jean Beltran PM, Ueno N, *et al*. Mechanical force induces phosphorylation-mediated signaling that underlies tissue response and robustness in xenopus embryos. Cell Syst. 2019;8(3):226-241.e7. DOI: 10.1016/j.cels.2019.01.006.
31. Rossy J, Laufer JM, Legler DF. Role of mechanotransduction and tension in T cell function. Front Immunol. 2018;9:2638,1-11. DOI: 10.3389/fimmu.2018.02638.
32. Harmening DM. Modern blood banking & transfusion practices. 7th ed. Philadelphia: F.A. Davis Company; 2019. pp: 333-354.
33. Protocol for isolating mononuclear cells from whole blood by density gradient centrifugation. STEMCELL Technologies [Internet]. [cited 2025 June 15]. Available from: https://www.stemcell.com/isolating-mononuclear-cells-from-whole-blood-by-density-gradient-centrifugation.html.
34. Imai Y, Chiba T, Kondo T, Kanzaki H, Kanayama K, Ao J, *et al*. Interferon-γ induced PD-L1 expression and soluble PD-L1 production in gastric cancer. Oncol Lett. 2020;20(3):2161-2168. DOI: 10.3892/ol.2020.11757.
35. Salmon P, Trono D. Production and titration of lentiviral vectors. Curr Protoc Neurosci. 2006; Chapter 4: Unit 4.21. DOI: 10.1002/0471142301.ns0421s37.
36. Han X, Bryson PD, Zhao Y, Cinay GE, Li S, Guo Y, *et al*. Masked chimeric antigen receptor for tumor-specific activation. Mol Ther. 2017;25(1):274-284. DOI: 10.1016/j.ymthe.2016.10.011.
37. Ito T, Ueno T, Clarkson MR, Yuan X, Jurewicz MM, Yagita H, *et al*. Analysis of the role of negative T cell costimulatory pathways in CD4 and CD8 T cell-mediated alloimmune responses *in vivo*. J Immunol. 2005;174(11):6648-6656. DOI: 10.4049/jimmunol.174.11.6648.
38. Tran CT, Wolz P, Egensperger R, Kösel S, Imai Y, Bise K, *et al*. Differential expression of MHC class II molecules by microglia and neoplastic astroglia: relevance for the escape of astrocytoma cells from immune surveillance. Neuropathol Appl Neurobiol. 1998;24(4):293-301. DOI: 10.1046/j.1365-2990.1998.00120.x.
39. Esensten JH, Helou YA, Chopra G, Weiss A, Bluestone JA. CD28 costimulation: from mechanism to therapy. Immunity. 2016;44(5):973-988. DOI: 10.1016/j.immuni.2016.04.020.
40. Kaufman HL, Deraffele G, Mitcham J, Moroziewicz D, Cohen SM, Hurst-Wicker KS, *et al*. Targeting the local tumor microenvironment with vaccinia virus expressing B7.1 for the treatment of melanoma. J Clin Invest. 2005;115(7):1903-1912. DOI: 10.1172/JCI24624.
41. Li B, Yang C, Jia G, Liu Y, Wang N, Yang F, *et al*. Comprehensive evaluation of the effects of long-term cryopreservation on peripheral blood mononuclear cells using flow cytometry. BMC Immunol. 2022;23(1):30,1-14. DOI: 10.1186/s12865-022-00505-4.
42. Repnik U, Knezevic M, Jeras M. Simple and cost-effective isolation of monocytes from buffy coats. J Immunol Methods. 2003;278(1-2):283-292. DOI: 10.1016/S0022-1759(03)00231-X.
43. Szczepiorkowski ZM, Burnett CA, Dumont LJ, Abhyankar SH. Apheresis buffy coat collection without photoactivation has no effect on apoptosis, cell proliferation, and total viability of mononuclear cells collected using photopheresis systems. Transfusion. 2018;58(4):943-950. DOI: 10.1111/trf.14532.
44. Dalton DK, Haynes L, Chu CQ, Swain SL, Wittmer S. Interferon gamma eliminates responding CD4 T cells during mycobacterial infection by inducing apoptosis of activated CD4 T cells. J Exp Med. 2000;192(1):117-122. DOI: 10.1084/jem.192.1.117.
45. Refaeli Y, Van Parijs L, Alexander SI, Abbas AK. Interferon gamma is required for activation-induced death of T lymphocytes. J Exp Med. 2002;196(7):999-1005. DOI: 10.1084/jem.20020666.
46. Li X, McKinstry KK, Swain SL, Dalton DK. IFN-γ acts directly on activated CD4+ T cells during mycobacterial infection to promote apoptosis by inducing components of the intracellular apoptosis machinery and by inducing extracellular proapoptotic signals. J Immunol. 2007;179(2):939-949. DOI: 10.4049/jimmunol.179.2.939.
47. Boulch M, Cazaux M, Cuffel A, Ruggiu M, Allain V, Corre B, *et al*. A major role for CD4+ T cells in driving cytokine release syndrome during CAR T cell therapy. Cell Rep Med. 2023;4(9):101161,1-11. DOI: 10.1016/j.xcrm.2023.101161.
48. Bos R, Sherman LA. $CD4^+$ T-cell help in the tumor milieu is required for recruitment and cytolytic function of $CD8^+$ T lymphocytes. Cancer Res. 2010;70(21):8368-8377. DOI: 10.1158/0008-5472.CAN-10-1322.
49. Prosser ME, Brown CE, Shami AF, Forman SJ, Jensen MC. Tumor PD-L1 co-stimulates primary human CD8(+) cytotoxic T cells modified to express a PD1:CD28 chimeric receptor. Mol Immunol. 2012;51(3-4):263-272. DOI: 10.1016/j.molimm.2012.03.023.
50. Rataj F, Kraus FBT, Chaloupka M, Grassmann S, Heise C, Cadilha BL, *et al*. PD1-CD28 fusion protein

enables CD4+ T cell help for adoptive T cell therapy in models of pancreatic cancer and non-Hodgkin lymphoma. Front Immunol. 2018;9:1955,1-12. DOI: 10.3389/fimmu.2018.01955.
51. Rajasekaran K, Xiong V, Fong L, Gorski J, Malarkannan S. Functional dichotomy between NKG2D and CD28-mediated co-stimulation in human CD8+ T cells. PloS One. 2010;5(9):e12635,1-10. DOI: 10.1371/journal.pone.0012635.
52. Dhar P, Wu JD. NKG2D and its ligands in cancer. Curr Opin Immunol. 2018;51:55-61. DOI: 10.1016/j.coi.2018.02.004.
53. Diefenbach A, Jensen ER, Jamieson AM, Raulet DH. Rae1 and H60 ligands of the NKG2D receptor stimulate tumour immunity. Nature. 2001;413(6852):165-171. DOI: 10.1038/35093109.
54. Schwinn N, Vokhminova D, Sucker A, Textor S, Striegel S, Moll I, *et al*. Interferon-gamma down-regulates NKG2D ligand expression and impairs the NKG2D-mediated cytolysis of MHC class I-deficient melanoma by natural killer cells. Int J Cancer. 2009;124(7):1594-1604. DOI: 10.1002/ijc.24098.
55. Lee SY, Lee DH, Sun W, Cervantes-Contreras F, Basom RS, Wu F, *et al*. CD8+ chimeric antigen receptor T cells manufactured in absence of CD4+ cells exhibit hypofunctional phenotype. J Immunother Cancer. 2023;11(11):e007803,1-14. DOI: 10.1136/jitc-2023-007803.
56. Ishii K, Pouzolles M, Chien CD, Erwin-Cohen RA, Kohler ME, Qin H, *et al*. Perforin-deficient CAR T cells recapitulate late-onset inflammatory toxicities observed in patients. J Clin Invest. 2020;130(10):5425-5443. DOI: 10.1172/JCI130059.
57. Zhao S, Wang C, Lu P, Lou Y, Liu H, Wang T, *et al*. Switch receptor T3/28 improves long-term persistence and antitumor efficacy of CAR-T cells. J Immunother Cancer. 2021;9(12):e003176,1-18. DOI: 10.1136/jitc-2021-003176.
58. Segal BM, Glass DD, Shevach EM. Cutting Edge: IL-10-producing CD4+ T cells mediate tumor rejection. J Immunol. 2002;168(1):1-4. DOI: 10.4049/jimmunol.168.1.1.
59. Zhao Y, Chen J, Andreatta M, Feng B, Xie YQ, Wenes M, *et al*. IL-10-expressing CAR T cells resist dysfunction and mediate durable clearance of solid tumors and metastases. Nat Biotechnol. 2024;42(11):1693-1704. DOI: 10.1038/s41587-023-02060-8.